Al-Azhar University Civil Engineering Research Magazine (CERM)
Vol. (39) No. (2) April, 2017

Strengthening of Eccentrically Loaded HSS Columns using CFRP Plates

Wael Attiah[1], Amr Shaat[2], Ezzeldin Sayed-Ahmed[3]

[1]*Department of Structural Engineering, Ain Shams University, Cairo, Egypt*
[2]*Civil Engineering Program, German University in Cairo, New Cairo, Egypt (On leave from Ain-Shams University)*
[3]*Construction Engineering Department, American University in Cairo, New Cairo, Egypt*
eysahmed@aucegypt.edu

ملخص

الأساليب التقليدية لتدعيم المنشآت الحديدية تحتوي على وصلات بمسامير أو لحام لألواح حديدية ثقيلة الوزن، وتتطلب هذه التقنيات التقليدية معدات رفع ثقيلة وأنظمة تدعيم أثناء التنفيذ والتي تؤدي إلى تأخر تنفيذ أعمال التدعيم وزيادة الأحمال الدائمة على المنشأ نتيجة لاستخدام الألواح الثقيلة. وكبديل فعال لهذه التقنيات يتم استخدام ألواح الألياف المدعمة بالبوليمرات وبصفة خاصه ألياف الكربون لامتلاكها نسبة جساءة إلى الوزن عالية، مع إمكانية استخدام ألياف الكربون المدعمة بالبوليمرات على الأسطح المنحنية والأسطح ذات الأشكال الهندسية المعقدة. هذه الورقة البحثية تقوم بدراسة العناصر الحديدية المدعمة عند تعريضها لحمل لامحوري ذات قيم مختلفة. ويهدف البحث إلى استكشاف سلوك العناصر المدعمة وتوصيف مقدار الزيادة قي مقاومة العناصر الإنشائية الحديدية ذات نسب نحافة مختلفة والمستخدم في تدعيمها ألياف الكربون المدعمة بالبوليمرات بتخانات مختلفة لألواح الألياف.

ABSTRACT

This paper investigates the behaviour of HSS beam-columns strengthened using CFRP plates. Finite element model was developed and verified against experimental results. A parametric study was carried out to examine the effect of a wide range of column slenderness ratios for HSS 64 X 64 X 3.2mm considering three eccentricity values in loading of half, one and twice the width of cross section. Also, the study examines the effect of different CFRP reinforcement ratios and their influence on the effectiveness of such strengthening system for HSS beam-columns. ANSYS software was adopted for numerical study. For material modelling, non-linearity of steel material was considered. The CFRP plates were treated as an orthotropic linear material. Cohesive zone feature was adopted to simulate the debonding of the CFRP plates from the steel tubes. HASHIN failure criteria was adopted to consider the progressive damage model for CFRP plates. The study shows significant increases in beam-column capacity and a reduction in member axial and lateral deformations depending on member's slenderness ratio and cross section with the effectiveness contribution of CFRP plates which is governed by the interfacial stresses developed in the adhesive layer.

KEYWORDS: HSS, steel, column, CFRP, eccentric, debonding

INTRODUCTION:

This paper aims to investigate behaviour of HSS beam-column (axial + Uniaxial bending moment) members and the suitability of using CFRP laminates to increase the capability of the cross section to sustain additional loads by increasing applied loads or due to maintain serviceability requirements would be serious for a the structure. To conduct this investigation, the study will begin to verify the finite element model with experimental works that have done for HSS under eccentric loading and for column

slenderness ratio of 120. Nine specimens were examined under three values of eccentricity 25, 50 and 100 mm, three control specimens (un-strengthened) one for each eccentricity value. The other two specimens are for strengthened specimens, the columns were fabricated using HSS section (48 x 48 x 2.0 mm). 40 mm CFRP wide and thickness of 1.4 mm strips were bonded longitudinally on each of the two opposite sides of all strengthened specimens. This paper introduces a numerical model to investigate behaviour and strength of CFRP strengthened HSS beam-columns considering different scenarios of failure modes whether due to debonding or rupture of CFRP laminates. After verifying the experimental works, a parametric study was carried out to examine the effect of a wide range of column slenderness ratios for HSS 64 X 64 X 3.2mm considering three eccentricity values in loading half, one and twice the width of cross section.

The Numerical Model

The numerical model was implemented using the finite element package (ANSYS, 16.2), and was applied to study the structural behavior of the eccentrically loaded carbon steel cold-formed HSS strengthened using bonded CFRP laminate oriented in the longitudinal direction [Figure 0-1]. The model considers two material models, bilinear stress – strain relationship for steel with yield strength measured experimentally and plastic tangential modulus equals 1/100 of elastic modulus (Et = Eelastic /100) and an orthotropic elastic relationships for CFRP laminates. The interaction between cold-formed HSS and CFRP laminate was also considered using cohesion model. Columns were modeled with 2.0mm thick shell elements. The hinged ends of the column were modeled as rigid end plates constrained to the specimen using rigid links simulate bolted connection. At bottom end, the translational degrees of freedom UX, UY, and UZ restrained along vertical line and to be adjusted accordingly to adopt required eccentricity, while degrees of freedom UX and UZ where restrained at top end [Figure 0-1].

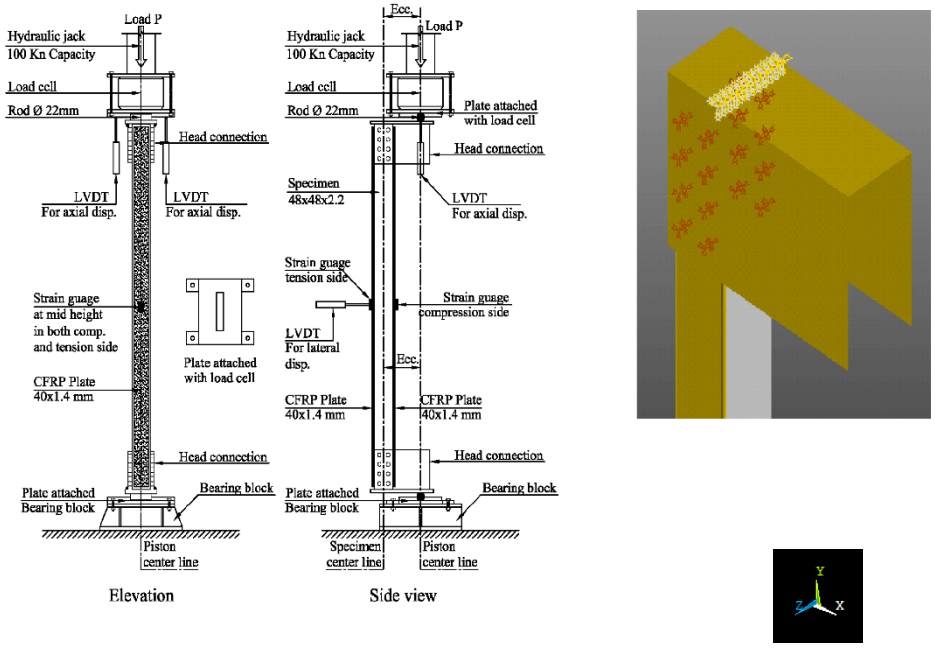

Figure 0-1 Experimental test setup and numerical model

Material Model

The material properties of steel plates were obtained through coupon tests which was carried out according to ASTM E8. The key results averaged from the three coupon tests shown and given in [**Error! Reference source not found.**] and [Table 0-1] respectively. The mechanical properties of CFRP laminates and epoxy resin are taken as given by the manufacture in their relative data sheets. A summary of material properties is shown in [Table 0-1].

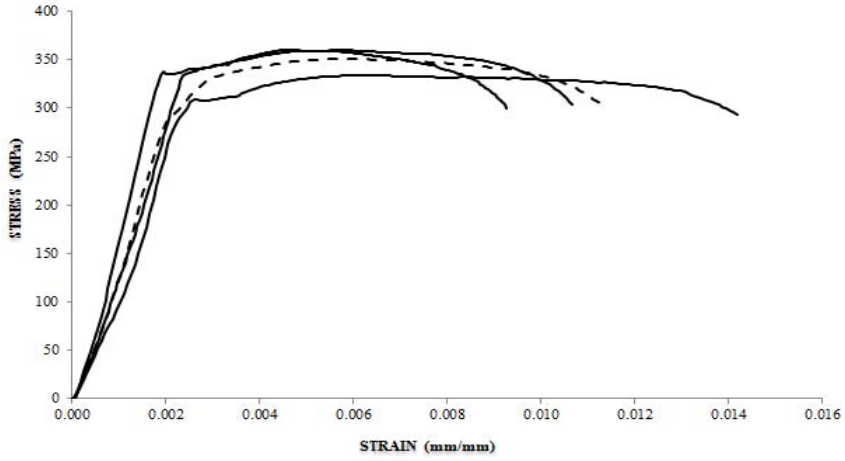

Figure 0-1 Test Specimens Results

Table 0-1 Mechanical Properties Steel Plates, CFRP & Epoxy

Material	E (MPa)	□y average (MPa)	□u (MPa)
STEEL PLATES	200000	335	350
CFRP (BASF MBRACE LAMINATE)	200000	N/A	2400
EPOXY RESIN (BASF MBRACE LAMINATE ADHESIVE)	10000	N/A	32

HSS - CFRP Interaction properties

HSS-CFRP adhesive layer was modelled using cohesive zone feature provided by (ANSYS, 16.2). The interface of delamination was introduced using contact elements. This approach introduces failure mechanisms by using the bi-linear hardening-softening relationships between the separations and incorporating the corresponding forces across the interface [Figure 0-1]. Debonding is governed by both interfacial normal stresses (mode I) and interfacial shear stresses (mode II). (Fernando, 2010) that predict a relation between peak bond stresses and the slippage of CFRP to steel interface at various levels of loading help in prediction of interfacial fracture energy from mechanical properties of the joint. Equations (4.1, 4.2, 4.3 & 4.4) are adopted for linear elastic adhesives that describe the progress of slippage at different stress levels. The bond-slip relation of CFRP-to-steel interfaces with a linear adhesive have bi-linear shape, the curve has an ascending part till slippage peak bond stress □max and slippage □□□the curve starts descending to reach zero shear bond stress and slippage □f as shown in [Figure 0-1]. For bond-separation model, the common method to get the bond-separation model and

to determine fracture energy is using double cantilever beam tests (Pardoen et al., 2005); (De Moura, M.F.S.F. and Chousal, J.A.G., 2006). In case of unavailability of these test data and for elastic linear adhesives, an approximation of the bond-separation model using the tensile stress-strain data of the adhesive can be used (Campilho et al., 2008). The peak stress of the bond-separation curve to be assumed similar to the tensile strength of the adhesive and the separation at complete failure δf can be taken as the product of the tensile strain at complete failure and the adhesive thickness (Campilho et al., 2008).

$G_f = 6\square\square\ t_a^{0.5}\ R^2$ (N/mm2.mm) (0.1)

$\square_{max} = 0.9\ \sigma_{max}$ (MPa) (0.2)

$\square_{\square}\square\square\square\square\square\square(\frac{t_a}{G_a})^{0.6}\sigma_{max}\square\square$mm) (0.3)

$\square_f\square\square\square\left(\frac{2G_f}{T_{max}}\right)\square\square$mm) (0.4)

Where:

t_a is the adhesive thickness in mm

R is the tensile strain energy of the adhesive which is equal to the area under the uni-axial tensile stress (in MPa) - strain curve. $R\square\square\square\left(\frac{\sigma^2 max}{2E_a}\right)\square$

σ_{max} Tensile strength of the adhesive (MPa).

G_a is the shear modulus of the adhesive layer (MPa).

In (Eid et al., 2016), the tensile strength of epoxy resin is equal to 32 MPa with an elastic modulus of 10 GPa. The traction – separation energy was calculated by following the bi-linear stress-strain curve introduced in [Figure 0-1]. The calculation of bi-linear stress-strain curve starts with ascending slope equals 10 GPa till the ultimate tensile stress of 32 MPa and the ultimate strain of 0.0032. To determine the bi-linear bond-separation relationship considering that the BASF epoxy resin is an elastic linear adhesive, the descending part of the relation ends with zero stress point and ultimate strain of 0.0064 which equals to twice the strain value at peak stress and form the completion of de-bonding energy. And regarding determination of bond-slip model, a study was conducted to calibrate (Fernando, 2010) model against test results carried out by (Eid et al., 2016), the study consider to find the best values for bond interfacial energy and peak bond stress that verify experiments ultimate loads and the observed failure modes tables will be Equations (4.5, 4.6, 4.7 & 4.8) show a good agreement in results for finite element models compared to their counter parts from test results as shown in [A parametric study was done on strengthened beam-column to evaluate the effect of different slenderness ratios that axially loaded considering three eccentricity values in loading half, one and twice the width of cross section on the increase of ultimate strength. Three slenderness ratios are adopted for the study 46, 70 and 93, this variation in slenderness ratio covers different type of columns ranged from stocky columns as 46 and 93 for slender columns. A high grade S355 HSS cold-formed steel columns with compact section 64 X 64 X 3.2mm and Fy = 355 MPa was specified for parametric study. High-modulus CFRP strips with E = 313 GPa and ultimate strength of 1475 MPa. Different separation-traction model was adopted in the study as shown in **Error! Reference source not found.**. The reinforcement ratio of CFRP plate area to

steel area is 0.232. **Error! Reference source not found.** shows the ultimate load capacities and percentage of increase for strengthened columns noting that, all strengthened specmens failed by debonding of CFRP plate. Figure 0-2 shows the different percentage of gain at various level of eccentricity value. As noted in the figure, the maximum gain effect of 53% occurs at lower eccentricity value of 32mm for slender column with KL/r = 93. The study shows that, the percentage of gain is inversely proportioned eccentricity value for long columns (KL/r 70 & 93) whereas it increased with the slenderness ratio of columns.

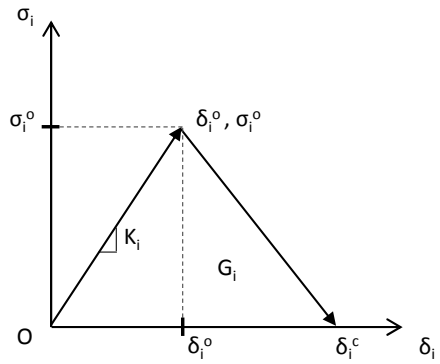

Fracture mode	Peak bond Traction/ stress σ_i^o (MPa)	Separation/ Slip δ_i^o at peak bond (mm)	Interfacial fracture energy, G_i (N/mm)
I	22.34	0.002	0.041
II	20.11	0.0013	1.031
III	20.11	0.0013	1.031

Figure 0-1 Traction-Separation model and values for cohesive zone model

Table 0-1 Parametric study specimens

Specimen	Ecc. (mm)	HSS length (mm)	Slender -ness ratio	CFRP		Ultimate load (KN) and Ratio	
				x-sec area mm2	Length (mm)	PFEA	PStrengthened PControl
C-46-32C	32	1122.2	46	-	-	119.01	-
S-46-32S	32	1122.2	46	86.0	1120	123.55	1.04
C-46-64C	64	1122.2	46	-	-	78.90	-
S-46-64S	64	1122.2	46	86.0	1120	83.57	1.06
C-46-128C	128	1122.2	46	-	-	46.07	-
S-46-128S	128	1122.2	46	86.0	1120	49.40	1.07
C-70-32C	32	1707.7	70	-	-	95.49	-
S-70-32S	32	1707.7	70	86.0	1705	120.87	1.22
C-70-64C	64	1707.7	70	-	-	65.82	-
S-70-64S	64	1707.7	70	86.0	1705	75.78	1.15
C-70-128C	128	1707.7	70	-	-	40.48	-
S-70-128S	128	1707.7	70	86.0	1705	43.73	1.08
C-93-32C	32	2268.8	93	-	-	76.90	-
S-93-32S	32	2268.8	93	86.0	2265	117.52	1.53
C-93-64C	64	2268.8	93	-	-	54.93	-
S-93-64S	64	2268.8	93	86.0	2265	74.65	1.38
C-93-128C	128	2268.8	93	-	-	35.49	-
S-93-128S	128	2268.8	93	86.0	2265	43.73	1.23

] with mean prediction ratio for ultimate loads of 1.02 and standard deviation of 0.11.

$G_f = 11\ t_a^{0.5}\ R^2$ (N/mm2.mm) (0.5)

$\tau_{max} = 0.375\ \sigma_{max}$ (MPa) (0.6)

$\delta_1 = 0.5\ \delta_f$ (mm) (0.7)

$\delta_f = \left(\frac{2G_f}{T_{max}}\right)$ (mm) (0.8)

The contribution of both normal and tangential contact stresses on the total fracture energy is considered via mixed-mode debonding. For mixed-mode debonding, both

normal and tangential contact stresses contribute to the total fracture energy and debonding is completed before the critical fracture energy values are reached for the components. Therefore, a power law based energy criterion is used to define the completion of debonding:

$$\left\{\frac{Gn}{Gcn}\right\} + \left\{\frac{Gt}{Gct}\right\} = 1$$

Where:

$G_n = \int P du_n$ and $G_t = \int \tau du_t$

τ: Tangential contact stress & P: Normal contact stress

G_n: the normal fracture energy. G_t: the tangential fracture energy

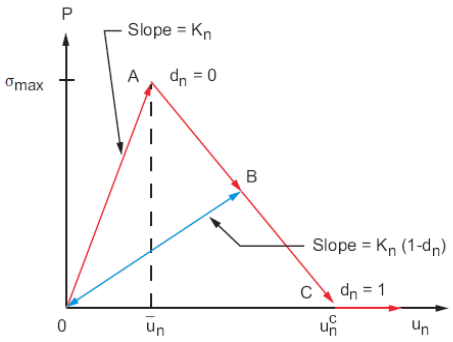

Fracture mode	Peak bond Stress (Mpa)	Separtion/Slippage @ peak stress (mm)	Fracture energy (N/mm2.mm)
I (normal separtion)	32	0.0064	0.1024
II (Long. Slippage)	12	0.0048	0.0288
III (Trans. Slippage)	12	0.0048	0.0288

Figure 0-1 Bi-Linear relationship between contact stress (Separation/Slippage) and contact gap

CFRP Damage Initiation and Propagation

Hashin failure criteria for unidirectional fiber composites was considered to onset material damage. The Hashin failure criterion proposes four separate modes of failure: Fiber tension, fiber compression, matrix tension and matrix compression. These failures are based on limiting material strengths in longitudinal tensile XTEN, longitudinal compressive XCMP, transverse tensile YTEN, transverse compressive YCMP and shear XY/YZ [

Table 0-1].

Table 0-1 Damage initiation strength limits

Loading Type	**Direction**		
	Longitudinal X	**Transversal Y**	**Transversal Z**
E (MPa)	200000	10000	10000
□□□Poisson Ratio)	0.2	0.02	0.02
Tensile Stress (MPa)	2400	50	50
Compressive Stress (MPa)	1440	250	250
Shear Stress (MPa)	77	77	77

The evolution of damage following the initiation of damage was based on Material Property Degradation Method (MPDG), which is an "instant stiffness reduction" setting a reduction factor of one as a complete damage for tension/compression loadings in all directions.

Verification of the Numerical Model

The FE results were compared with the experimental research data published by (Eid et al., 2016) to verify the model before using it in the parametric study.[Table 0-1] summarizes the load capacities obtained from the FE models of control specimen (C120) and the strengthened specimen (S120). The finite element ultimate strength PFEM matched well with the experimental ultimate load PExp showing a variation of about 6%. The strengthened columns failed due to debonding of the CFRP layer on the compression side of the buckled column.

Table 0-1 Summary of the FE and Experimental results

Specimen	Ecc. Mm	HSS length mm	Slender - ness ratio	CFRP		Ultimate load KN		Ratio
				x-sec area mm^2	Length mm	P_{Exp}	P_{FEA}	P_{Exp} / P_{FEA}
C-120-25C	25	2364	120	-	-	25.8	25.75	1.00
S-120-25 S	25	2364	120	56.0	2350	41.3	39.09	1.06
C-120-50C	50	2364	120	-	-	20.4	19.2	1.06
S-120-50S	50	2364	120	56.0	2350	31.7	30.2	1.05
C-120-100C	100	2364	120	-	-	13.7	13.2	1.04
S-120-100S	100	2364	120	56.0	2350	21.3	22.13	0.96

Parametric Study

A parametric study was done on strengthened beam-column to evaluate the effect of different slenderness ratios that axially loaded considering three eccentricity values in loading half, one and twice the width of cross section on the increase of ultimate strength. Three slenderness ratios are adopted for the study 46, 70 and 93, this variation in slenderness ratio covers different type of columns ranged from stocky columns as 46 and 93 for slender columns. A high grade S355 HSS cold-formed steel columns with compact section 64 X 64 X 3.2mm and Fy = 355 MPa was specified for parametric study. High-modulus CFRP strips with E = 313 GPa and ultimate strength of 1475 MPa. Different separation-traction model was adopted in the study as shown in **Error! Reference source not found.**. The reinforcement ratio of CFRP plate area to steel area is 0.232. **Error! Reference source not found.** shows the ultimate load capacities and percentage of increase for strengthened columns noting that, all strengthened specmens failed by debonding of CFRP plate. Figure 0-2 shows the different percentage of gain at various level of eccentricity value. As noted in the figure, the maximum gain effect of 53% occurs at lower eccentricity value of 32mm for slender column with KL/r = 93. The study shows that, the percentage of gain is inversely proportioned eccentricity value for long columns (KL/r 70 & 93) whereas it increased with the slenderness ratio of columns.

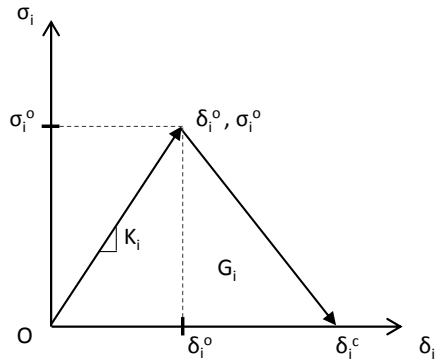

Fracture mode	Peak bond Traction/ stress σ_i^o (MPa)	Separation/ Slip δ_i^o at peak bond (mm)	Interfacial fracture energy, G_i (N/mm)
I	22.34	0.002	0.041
II	20.11	0.0013	1.031
III	20.11	0.0013	1.031

Figure 0-1 Traction-Separation model and values for cohesive zone model

Table 0-1 Parametric study specimens

Specimen	Ecc. (mm)	HSS length (mm)	Slender -ness ratio	CFRP		Ultimate load (KN) and Ratio	
				x-sec area mm^2	Length (mm)	P_{FEA}	$P_{Strengthened}$ / P_{Contr}
C-46-32C	32	1122.2	46	-	-	119.01	-
S-46-32S	32	1122.2	46	86.0	1120	123.55	1.04
C-46-64C	64	1122.2	46	-	-	78.90	-
S-46-64S	64	1122.2	46	86.0	1120	83.57	1.06
C-46-128C	128	1122.2	46	-	-	46.07	-
S-46-128S	128	1122.2	46	86.0	1120	49.40	1.07
C-70-32C	32	1707.7	70	-	-	95.49	-
S-70-32S	32	1707.7	70	86.0	1705	120.87	1.22
C-70-64C	64	1707.7	70	-	-	65.82	-
S-70-64S	64	1707.7	70	86.0	1705	75.78	1.15
C-70-128C	128	1707.7	70	-	-	40.48	-
S-70-128S	128	1707.7	70	86.0	1705	43.73	1.08
C-93-32C	32	2268.8	93	-	-	76.90	-
S-93-32S	32	2268.8	93	86.0	2265	117.52	1.53
C-93-64C	64	2268.8	93	-	-	54.93	-
S-93-64S	64	2268.8	93	86.0	2265	74.65	1.38
C-93-128C	128	2268.8	93	-	-	35.49	-
S-93-128S	128	2268.8	93	86.0	2265	43.73	1.23

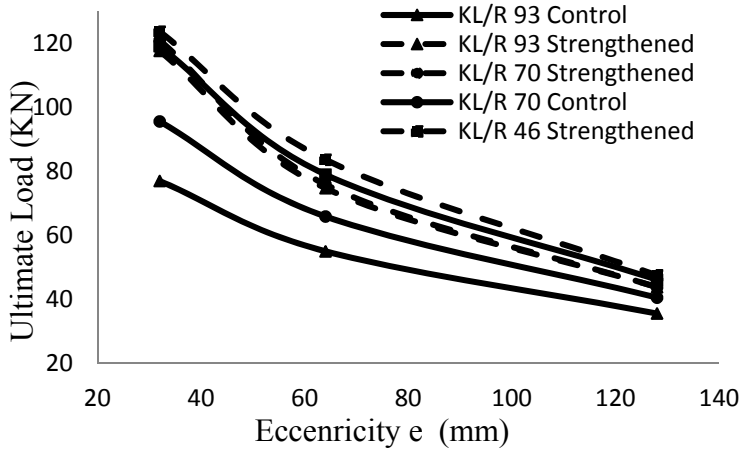

Figure 0-2 % Percentage of gain and Eccentricity value

Conclusion

In this numerical analysis study, a finite element model was created and verified against experimental test results done by (Eid et al., 2016) for HSS slender beam-columns strengthened with CFRP plates. After the verification of the model, a parametric study was performed to investigate the effect of slenderness ratio and load eccentricity on the gain in strength resulted from the strengthening system. The study shows that for high eccentricity value, the percentage of gain decreased compared to lower value for the same column except for short columns that typically failed be yield of cross-section not buckling. The percentage gain ranged from %3 to %53. Also, the study reveals that for more slender column (KL/r=93) the strengthening system will be more efficient.

References

[1] ANSYS, 16.2. *ANSYS mechanical APDL structural analysis guide, release 16.2, 2015.*

[2] Campilho et al. (2008). "Using a cohesive damage model to predict the tensile behaviour of CFRP single strap repairs". *International Journal of Solids and Structures, 45(5), 1497-1512*.

[3] De Moura, M.F.S.F. and Chousal, J.A.G. (2006). "Cohesive and continuum damage models applied to fracture characterization of bonded joints". *International Journal of Mechanical Sciences, 48(5), 493-503.*

[4] Eid et al. (2016). CFRP-Strengthening of Eccentrically Loaded HSS Steel Columns. *Proceedings of the Second International Conference on Infrastructure Management, Assessment and Rehablitation Techniques.*

[5] Fernando, N. D. (2010). *BOND BEHAVIOUR AND DEBONDING FAILURES IN CFRP-STRENGTHENED STEEL MEMBERS.* A Thesis Submitted in Partial Fulfilment of the Requirements forthe Degree of Doctor of Philosophy.

[6] Pardoen et al. (2005). "Constraint effects in adhesive joint fracture". *Journal of the Mechanics and Physics of Solids,53(9), 1951-1983*.